

Controlling carbon nanotube photoluminescence using silicon microring resonators

Adrien Noury, Xavier Le Roux, Laurent Vivien and Nicolas Izard

Institut d'Electronique Fondamentale, CNRS-UMR 8622, Univ. Paris-Sud, 91405 Orsay, France

E-mail: nicolas.izard@u-psud.fr

Abstract. We report on coupling between semiconducting single-wall carbon nanotubes (s-SWNT) photoluminescence and silicon microring resonators. Polyfluorene extracted s-SWNT deposited on such resonators exhibit sharp emission peaks, due to interaction with the cavity modes of the microring resonators. Ring resonators with radius of $5\ \mu\text{m}$ and $10\ \mu\text{m}$ were used, reaching quality factors up to 4000 in emission. These are among the highest values reported for carbon nanotubes coupled with an integrated cavity on silicon platform, which open up the possibility to build s-SWNT based efficient light source on silicon.

1. Introduction

Among today's carbon based nanomaterials, semiconducting carbon nanotubes (s-SWNT) stand out with their strong luminescence properties, and various potential applications have been proposed, such as optoelectronics and biosensing. Interestingly, s-SWNT direct bandgap could be tuned by adjusting their chiral index, and photoluminescence (PL) of well isolated individual s-SWNT was extensively studied, either by suspension over trenches and pillars [1,2] or encapsulation in micelle surfactant [3,4].

PL was also observed in an ensemble of s-SWNT [5], and more recently in composite-like materials where nanotubes are dispersed into a gelatin [6] or a polymer matrix [7,8], opening the route towards device fabrication. Furthermore, it is possible to stretch and align nanotubes dispersed in the matrix to enhance their PL properties [7,9].

However, even for polyfluorene-wrapped s-SWNT which display strong PL [8,10], the quantum efficiency remains low [11], which may put a brake on photonic applications. From this point, it is particularly attractive to couple s-SWNT PL with optical resonators [12], for PL enhancement and control of spontaneous emission through Purcell effect [13].

First reports of s-SWNT PL coupling with optical resonators used planar cavities, either using metallic mirror [14], dielectric mirror [15], or both [16].

More recent works took advantages of the Silicon-On-Insulator (SOI) platform to couple s-SWNT PL to suspended photonic crystal cavities [17,18], or silicon microdisk resonators [19]. An advantage of this approach is the integration with silicon photonics technology, even if it remains challenging to efficiently couple these structures with waveguides. On the other hand, we recently proposed an integration scheme to couple s-SWNT PL to silicon waveguides, using evanescent wave from narrow waveguides [20].

We propose to go further by coupling s-SWNT with microring resonators. Silicon microrings present various advantages for coupling with carbon nanotubes. Intrinsically, they are traveling-wave resonators, the optical wave being guided along the circumference of the ring, and light is efficiently loaded and extracted with silicon waveguides, as described by the coupled mode theory [21]. Moreover, the pace between two successive resonant peaks of the cavity, or Free Spectral Range (FSR), can be easily tuned by adjusting the ring diameter, making it easy to match s-SWNT emission wavelengths. At last, microring resonators on SOI substrate are known to exhibit quite high quality factor [22], turning them into an ideal candidate for carbon nanotube integration with silicon photonics.

Here, we report on the coupling of s-SWNT PL in silicon microring resonators. Polyfluorene-wrapped s-SWNT are deposited on top of the photonic structure to form a very thin homogeneous layer of a few nanometers thick. We observed sharp peaks regularly spaced and superimposed to s-SWNT broad emission peaks. These sharp peaks were attributed to s-SWNT PL coupled to microring resonators. We have observed quality factor as high as 4000, and we also demonstrate tuning of the cavity resonance

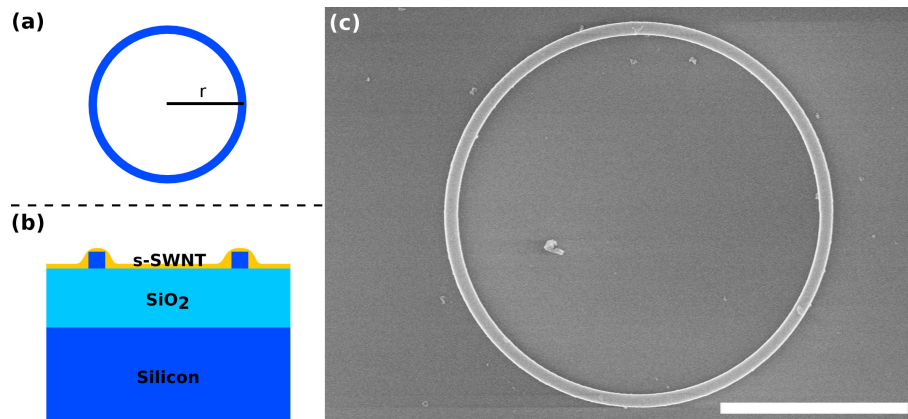


Figure 1. (a) Top view of a microring resonator of radius r . (b) Cross-section of the microring, with polyfluorene-wrapped s-SWNT top layer (not to scale). (c) Scanning electron micrograph of as-fabricated microring, with a radius r of $5 \mu\text{m}$. The scale bar is $5 \mu\text{m}$.

by changing the ring diameter.

2. Experimental details

The ring resonators are fabricated from SOI wafers with a 220 nm thick top Si layer and a $2 \mu\text{m}$ thick buried oxide layer. Electron beam lithography (NanoBeam nB4, 80 kV, 2.1 nA, step size 5 nm) is used to define the microring and silicon waveguides. A dry etching process with an inductively coupled plasma etcher ($\text{SF}_6/\text{C}_4\text{F}_8$) transfers the patterns in the top Si layer. The microring resonator was made from a 350 nm wide waveguide bended to form a circle. We used two different rings radius: $5 \mu\text{m}$ and $10 \mu\text{m}$. The microring was coupled to a strip waveguide of the same width, at a gap distance L_c of 85 nm between ring and waveguide. A schematic view of the microring is shown in figures 1(a) and 1(b), while a scanning electron micrograph of a typical microring prior to nanotube deposition is shown in figure 1(c).

Polyfluorene-wrapped s-SWNT were prepared from carbon nanotubes produced with the HiPCO process [23] (Unydim), using Poly-9,9-di-n-octyl-fluorenyl-2,7-diyl (PFO) (Sigma-Aldrich) in toluene as an extracting agent. Using ultracentrifugation up to 150000 g for 1 h, it is known that this process leads to well isolated PFO-wrapped s-SWNT displaying good electrical [24], optical [10] and electro-optical [25] properties. PFO/s-SWNT are deposited by spin casting (1000 rpm, 60 s) followed by thermal annealing of 30 min at 180°C

3. Results and discussions

First, the fabricated microring resonators are characterized prior to s-SWNT deposition. A strip waveguide is localized within coupling distance near to a microring. When light is injected into the waveguide, part of the energy will be coupled into the ring, before being

coupled back to the waveguide. For some given wavelengths depending on the microring dimensions - radius and width of the bended waveguide - resonances are observed, which appears as drop in transmittance. Therefore, the transmission spectrum is characterized by sharp absorption peaks. Figure 2(a) displays a typical transmission spectrum for a 10 μm radius microring in TE polarization. A typical resonance is highlighted in the inset and presents a symmetrical Lorentzian lineshape. A Lorentzian fit gives a Q -factor of approximately 4500, for a Full-Width Half Maximum about 290 pm.

Silicon microring resonators are also described by their Free Spectral Range (FSR), given by:

$$\Delta\lambda = \frac{\lambda^2}{n_g \cdot L}$$

where λ is the wavelength, n_g the group index and L the length of the optical resonator. We found a FSR ranging from 6.18 nm at 1283.65 nm to 7.26 nm at 1383.21 nm. The corresponding n_g is equal to 4.2, which is in complete adequation with the value of n_g expected for these kind of structures, as calculated with a mode solver (not shown).

Polyfluorene wrapped s-SWNT were deposited on top of the resonators by spin casting, and were subsequently annealed for 30 min at 180°C. The s-SWNT layer thickness was estimated by AFM and spectroscopic ellipsometry to be in the order of 5 nm (not shown). Deposition of s-SWNT induces drastic changes in microring resonators transmission as displayed in figure 2(b). The overall transmission decreases, and this is more pronounced at shorter wavelengths. This effect can be interpreted as, first, a change of light confinement due to the s-SWNT layer's presence (change in the cladding refractive index), effect which is more pronounced at lower wavelengths, and secondly, additional absorption due to the broad (8,7) s-SWNT absorption bands at these shorter wavelengths.

Moreover, the intensity of microring resonances significantly decreases. Positions of these resonances are highlighted by triangle marks (\blacktriangle) as a visual guide. A typical resonance is displayed in the inset. Although the intensity strongly decreases, the lineshape remains symmetrical and can be fitted by a Lorentzian, once the general linear trend is taken into account. The Lorentzian fit gives a Q -factor around 2200. Interestingly, the positions of these resonances and the FSR slightly changes compared to before s-SWNT deposition (FSR equal to 5.3 nm at 1283.96 nm), which was expected for a PFO based upper cladding.

Typical PL spectra of PFO-wrapped s-SWNT are displayed in figure 2(c). The pumping wavelength was 735 nm, and s-SWNT's PL spectra were recorded on glass (dark) and SOI (bright) substrates. The figure 2(c) inset displays PL spectrum of PFO-wrapped s-SWNT suspension in toluene for reference. Indexation of this PL spectrum was done based on previous works [8, 25]. Due to the silicon structure bandpass, the (8,7) s-SWNT is the main species interacting with microrings. It can be noticed that the short wavelength region on SOI substrate is dominated by the silicon PL tail. However, the (8,7) emission peak is clearly observed.

Using our home-built μ -PL setup, s-SWNT emission on top of microring resonators

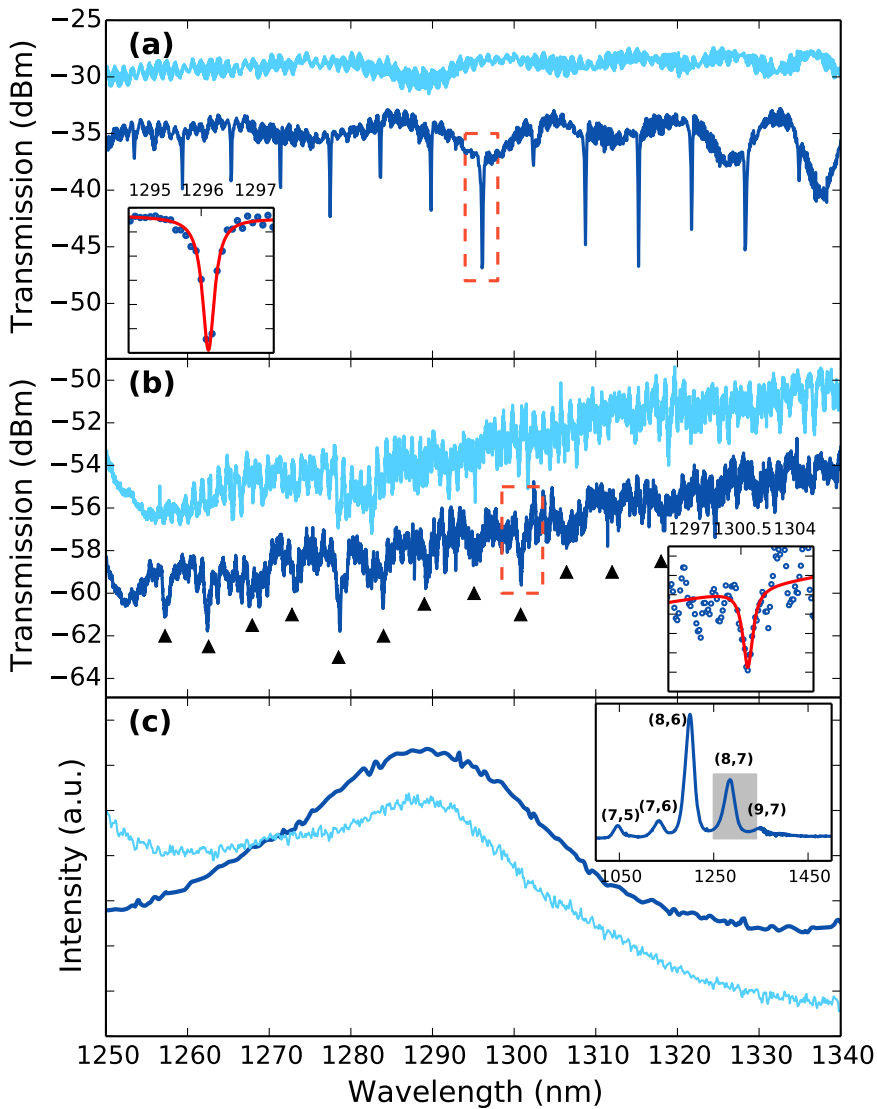


Figure 2. (a) Transmission spectra in TE polarization of a typical $10\ \mu\text{m}$ radius microring resonator coupled to a strip waveguide (dark) and a reference strip waveguide (bright). The reference was upshifted by 5 dBm for clarity. Depending on the wavelength, the distance between two resonant peaks (FSR) is comprised between 6 to 7 nm (see details in text). Inset depicts a close view of one of the resonance, fitted with a Lorentzian lineshape (solid line). (b) Linear transmission of a similar microring resonator (dark) and reference waveguide (bright), after s-SWNT deposition. The reference was again upshifted by 5 dBm for clarity. Dark triangles (\blacktriangle) are guides to the eye to underline resonant peaks positions. The FSR slightly increases after s-SWNT deposition. Inset: detailed view of an individual resonance. (c) Typical PL spectrum of s-SWNT after deposition on glass (dark) and SOI substrate (bright). In case of SOI substrate, the short wavelength region is dominated by silicon substrate PL tail. Inset shows the full band spectrum of s-SWNT in liquid with indexation, at an excitation wavelength of 735 nm.

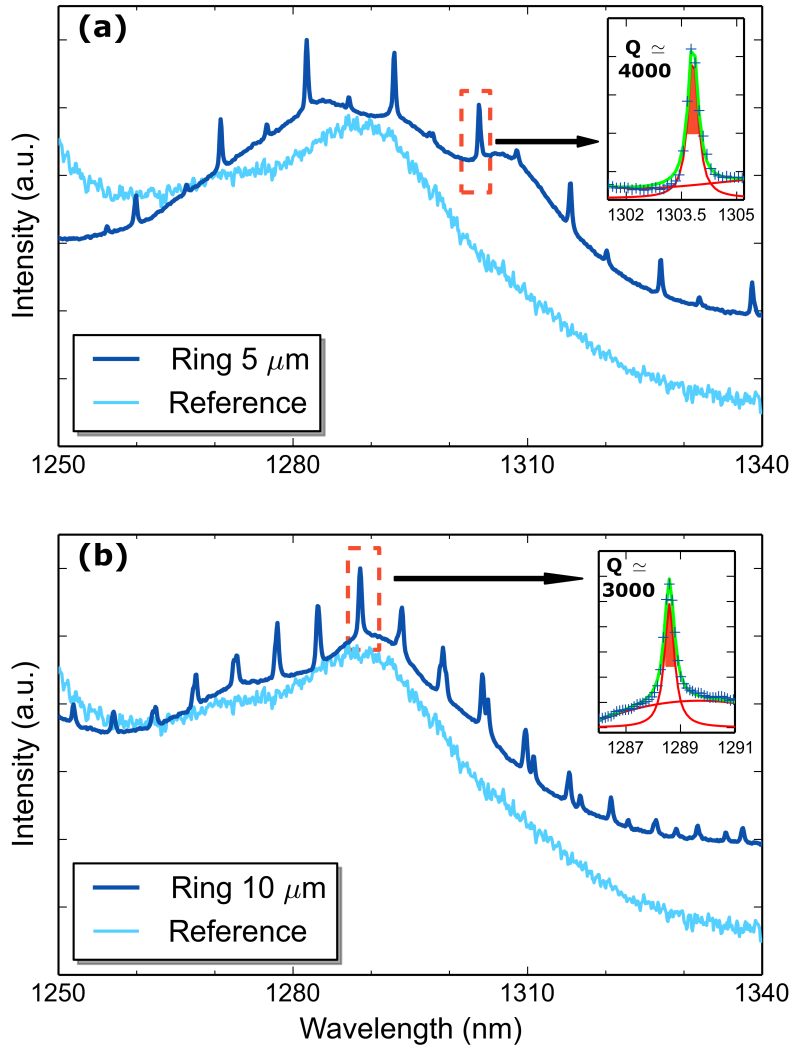


Figure 3. (a) Typical μ -PL spectra of a 5 μm microring resonator (dark) and reference outside the microring (bright). (b) Same with a 10 μm microring. Insets show typical Lorentzian fits giving the Q -factor. In this case, FWHM is 322 pm and the center wavelength is 1303.8 nm for the 5 μm microring, while the FWHM is 436 pm and the center wavelength is 1288.6 nm for the 10 μm microring. Excitation wavelength is 735 nm.

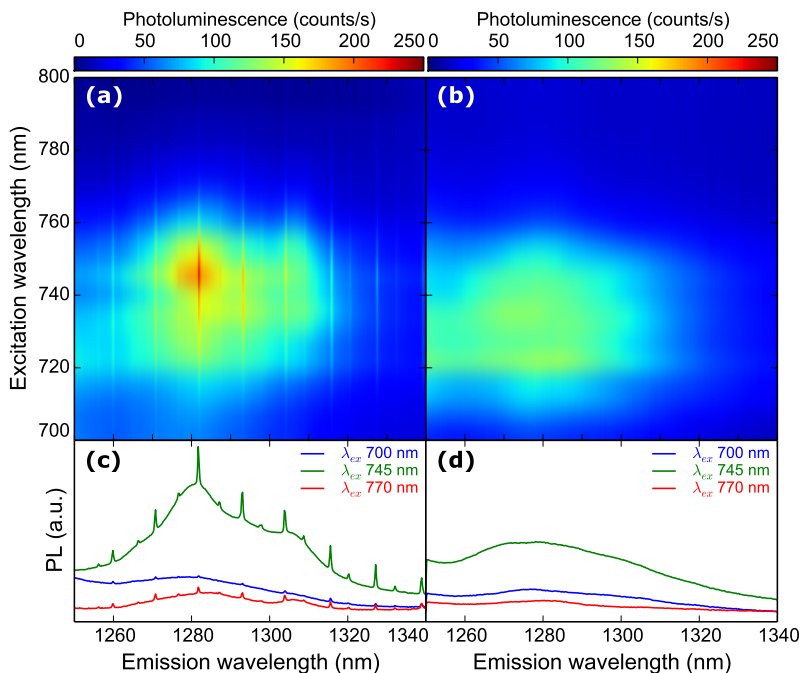


Figure 4. Top[(a), (b)] PLE map, and bottom[(c), (d)] corresponding PL spectra at different wavelengths for, respectively, a 5 μm microring resonator [left (a), (c)] and the reference substrate [right (b), (d)]. The peak centered around 1290 nm is attributed to (8,7) s-SWNT, while the signal on the edge at 1250 nm is attributed to the (8,6) and Si PL tail.

is measured. The output of a titanium-sapphire laser at 735 nm is focused onto the sample with an infrared microscope objective of 0.6 numerical aperture. PL is collected by the same objective, and the direct laser line is rejected by a dichroic beam splitter and a longpass filter. PL is recorded with a 320-mm spectrometer and 950 lines/mm grating, and detection is performed by a nitrogen-cooled 512-pixel linear InGaAs array. In this configuration, spot size diameter on top of silicon microrings was 15 μm , and the exciting power was maintained below 5 mW.

Typical results for 5 and 10 μm radius ring resonators are displayed in figures 3(a) and (b), respectively. The most striking feature is the appearance of sharp peaks regularly spaced, superimposed to the (8,7) s-SWNT broad emission peak. Their quality factors Q range mostly from 3000 to 4000. These sharp peaks are attributed to nanotube PL coupled to the microring whispering gallery mode. Part of the light emitted by the nanotube is directly collected by the microscope objective, resulting in the broad emission peak. However, a significant fraction of the energy couples to the microcavity modes: at resonant wavelengths, light emitted by the s-SWNT loads into the microring cavity. Intrinsic resonator losses induce far-field radiation, resulting in enhanced emission at these wavelengths compared to off resonance s-SWNT emission.

As the FSR directly depends on the microring radius, it is therefore expected that if the microring radius doubles (e.g. from 5 μm radius to 10 μm radius), the FSR will be halved. In figure 3(a) the FSR around 1290 nm is between 10 to 11 nm, while in

figure 3(b), the FSR is equal to 5.3 nm, which unambiguously proves that these sharp peaks can be attributed to microring resonances (with the FSR being of the same order as determined by linear transmission).

Moreover, the intensity of the microring peaks is modulated by the broad s-SWNT PL, the intensity of the peak being higher when the SWNT peak intensity is high. (cf. Supplementary Materials). This is another demonstration that these resonance peaks originate from s-SWNT PL coupled into the microring resonators.

For the 5 μm and 10 μm microring resonator, an additional serie of peaks is observed, with a lower intensity and a different FSR than the main serie. Although it is difficult to unambiguously assign these peaks, they might origin from TE/TM polarization, the low intensity set being attributed to TM modes.

To further investigate the coupling between s-SWNT and microring resonators, photoluminescence excitation (PLE) spectroscopy was performed (cf. figure 4). A striking feature of PLE map performed on top of microring resonators is the presence of sharp vertical peaks, disappearing when the (8,7) s-SWNT PL intensity drop. This effect is clearly unobserved when PLE map is performed outside the microring (figures 4(b) and (d)). These results again demonstrate that s-SWNT PL is well coupled into silicon microring, resulting in sharp emission peaks at the microring resonance.

4. Conclusion

In conclusion, we have demonstrated the coupling of s-SWNT PL in silicon microring resonators, resulting in sharp and regularly spaced emission peaks. The Free Spectral Range of these emission peaks could be easily tuned by adjusting the microring diameter. The quality factor Q of these emission peaks range from 3000 to 4000, which is among the highest values reported for integrated silicon cavities coupled to carbon nanotubes. Our results open up a range of possibilities for future photonic circuits, due to the straightforward coupling between silicon microring and strip waveguide [22] and their integration into more complex devices. For instance, recent results suggest that carbon nanotubes network could be electrically-driven to produce light in telecom wavelengths range, light originating from black body emission [26]. Coupled with silicon microring resonators into more complex devices, this could be the first step towards the implementation of on-chip light multiplexing. Additionally, enhanced localization of light in photonic crystal can increase significantly the interaction between s-SWNT PL and the propagating optical modes, leading to strong photoluminescence signal in such devices [27].

Acknowledgments

A. Noury acknowledges the Ministry of Higher Education and Research (France) for scholarship. The authors acknowledge C. Caër and A. Degiron for assistance and fruitful discussions. This work was supported by ANR JCJC project "Ça (Re-) Lase !" and

partly by the FET project "Cartoon". Fabrication was performed in the IEF clean room facilities (CTU/MINERVE), part of the RENATECH network.

References

- [1] J. Lefebvre, Y. Homma, and P. Finnie. *Phys. Rev. Lett.*, 90:217401, 2003.
- [2] J. Chen, V. Perebeinos, M. Freitag, J. Tsang, Q. Fu, J. Liu, and P. Avouris. *Science*, 310:1171, 2005.
- [3] M. J. O'Connell, S. M. Bachilo, C. B. Huffman, V. C. Moore, M. S. Strano, E. H. Haroz, K. L. Rialon, P. J. Boul, W. H. Noon, C. Kittrell, J. Ma, R. H. Hauge, R. B. Weisman, and R. E. Smalley. *Science*, 297:593, 2002.
- [4] A. Högele, C. Galland, M. Winger, and A. Imamoglu. *Phys. Rev. Lett.*, 100:217401, 2008.
- [5] S. Berger, C. Voisin, G. Cassabois, C. Delalande, and P. Roussignol. *Nano Lett.*, 7:398, 2007.
- [6] S. Berger, F. Iglesias, P. Bonnet, C. Voisin, G. Cassabois, J.-S. Lauret, C. Delalande, and P. Roussignol. *J. Appl. Phys.*, 105:094323, 2009.
- [7] C. Zamora-Ledezma, C. Blanc, and E. Anglaret. *Phys. Rev. B*, 80:113407, 2009.
- [8] E. Gauffrès, N. Izard, L. Vivien, S. Kazaoui, D. Marris-Morini, and E. Cassan. *Opt. Lett.*, 34:3845, 2009.
- [9] C. Zamora-Ledezma, C. Blanc, and E. Anglaret. *J. Phys. Chem. C*, 116:13760, 2012.
- [10] E. Gauffrès, N. Izard, X. Le Roux, D. Marris-Morini, S. Kazaoui, E. Cassan, and L. Vivien. *Appl. Phys. Lett.*, 96:231105, 2010.
- [11] Y. Miyauchi, H. Hirori, K. Matsuda, and Y. Kanemitsu. *Phys. Rev. B*, 80:081410(R), 2009.
- [12] K. J. Vahala. *Nature*, 424:839, 2003.
- [13] E.M. Purcell. *Phys. Rev.*, 69:681, 1946.
- [14] F. Xia, M. Steiner, Y.-M. Lin, and P. Avouris. *Nature Nanotech.*, 3:609, 2008.
- [15] E. Gauffrès, N. Izard, X. Le Roux, S. Kazaoui, D. Marris-Morini, E. Cassan, and L. Vivien. *Opt. Express*, 18:5740, 2010.
- [16] D. Legrand, C. Roquelet, G. Lanty, P. Roussignol, X. Lafosse, S. Bouchoule, E. Deleporte, C. Voisin, and J.S. Lauret. *Appl. Phys. Lett.*, 102:153102, 2013.
- [17] R. Watahiki, T. Shimada, P. Zhao, S. Chiashi, S. Iwamoto, Y. Arakawa, S. Maruyama, and Y. K. Kato. *Appl. Phys. Lett.*, 101:141124, 2012.
- [18] H. Sumikura, E. Kuramochi, H. Taniyama, and M. Notomi. *Appl. Phys. Lett.*, 102:231110, 2013.
- [19] S. Imamura, R. Watahiki, R. Miura, T. Shimada, and Y. K. Kato. *Appl. Phys. Lett.*, 102:161102, 2013.
- [20] E. Gauffrès, N. Izard, A. Noury, X. Le Roux, G. Rasigade, A. Beck, and L. Vivien. *ACS Nano*, 6:3813, 2012.
- [21] A. Yariv. *IEEE J. Quant. Electron.*, 9:919, 1973.
- [22] J. Niehusmann, A. Vörckel, P. H. Bolivar, T. Wahlbrink, W. Henschel, and H. Kurz. *Opt. Lett.*, 29:2861, 2004.
- [23] P. Nikolaev, M.J. Bronikowski, R.K. Bradley, F. Rohmund, D.T. Colbert, K.A. Smith, and R.E. Smalley. *Chem. Phys. Lett.*, 313:91, 1999.
- [24] N. Izard, S. Kazaoui, K. Hata, T. Okazaki, T. Saito, S. Iijima, and N. Minami. *Appl. Phys. Lett.*, 92:243112, 2008.
- [25] N. Izard, E. Gauffrès, X. Le Roux, S. Kazaoui, Y. Murakami, D. Marris-Morini, E. Cassan, S. Maruyama, and L. Vivien. *Eur. Phys. J. Appl. Phys.*, 55:20401, 2011.
- [26] M. Fujiwara, D. Tsuya, and H. Maki. *Appl. Phys. Lett.*, 103:143122, 2013.
- [27] C. Caër, X. Le Roux, and C. Cassan. *Appl. Phys. Lett.*, 103:251106, 2013.